BY-PASS TRANSITION TO AIRFOIL FLUTTER BY TRANSIENT GROWTH DUE TO GUST IMPULSE

M. Schwartz, P. Hémon, E. de Langre
LadHyX, Ecole Polytechnique – CNRS, F-91128 PALAISEAU, France

ABSTRACT

We present an experimental study which shows that a mechanism, known as transient growth of energy, can cause flutter instability of a non linearly flexible airfoil at a wind velocity below the linear critical flutter velocity. A flap mounted upstream a flexible airfoil in a wind tunnel generates a turbulent gust which triggers the oscillations. For the first time an experimental evidence is provided to confirm the theoretical scenario of a by-pass transition to flutter by transient growth. From an engineering point of view, transient growth might explain the premature structural fatigue encountered in structures subjected to wind.

1. INTRODUCTION

In linear flutter studies, it is common to assume that the system amplitude behaves exponentially in time, decaying or growing depending on the wind velocity U. The analysis then follows a normal modes approach where the long time behaviour is sought, particularly the critical value of the wind velocity U_c which determines the limit between stable and unstable behaviour.

However it has been shown by Schmid and de Langre (2003) that it is possible to observe a transient instability at a velocity below the critical velocity. In a linear case this mechanism leads initially to an amplification of the energy of the system that subsequently decreases due to stable conditions. This is called transient growth of energy. It is a consequence of non-orthogonal modes involved in the system (Schmid & Hennigson 2001). Transient growth depends strongly of the initial conditions produced by the initial perturbation. An experimental evidence of transient growth was given by Hémon et al. (2006) for a linearly flexible airfoil in a wind tunnel.

In a non linear case, the amplitude of the perturbation is an important parameter due to the subcritical branch. As shown in Figure 1, a small perturbation just below the linear critical velocity let the system in the stable region. As the initial perturbation is larger, the system state may reach the unstable region, leading to flutter even below U_c. This scenario is called by-pass transition to flutter.

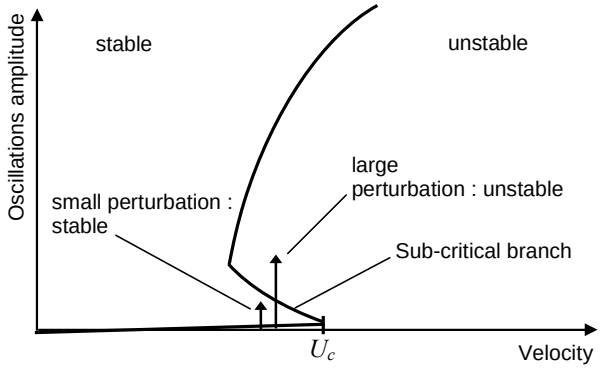

Figure 1: *Perturbation amplitude effect for a non-linear system: by-pass transition to flutter.*

But there is another possible scenario in which an initial small perturbation can be amplified by transient growth. As shown in Figure 2, if the amplification is such that the system response reaches the subcritical branch, then flutter instability is triggered. This is also a by-pass transition to flutter, caused by transient growth. The objective of the paper is to present for the first time an experimental study that confirms this theoretical scenario.

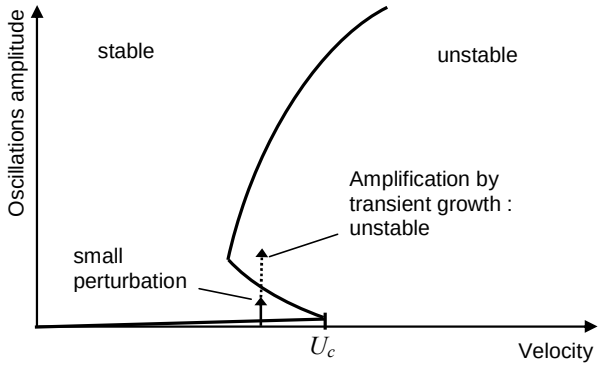

Figure 2: *Scenario of by-pass transition due to transient growth of an initial perturbation.*

Previous experimental studies have already deal

with non linear airfoil flutter, for instance by Marsden and Price (2005), but none of them have emphasized their study on the transient behaviour of such a system. Numerically, Lee et al. (2005) have focused their investigation on the mechanisms leading to limit cycle oscillations. They mainly investigated the supercritical velocity range although they mention "strong energy exchange between modes" at subcritical velocities, which could be interpreted as transient growth of energy.

We present first the experimental setup and the identification of nonlinear airfoil parameters. Then the results are presented in order to confirm the existence of the by-pass transition to flutter due to transient growth.

2. EXPERIMENTAL TECHNIQUES

2.1 Experimental setup

A NACA 0015 profile made of plexiglas is mounted in the test section of a small Eiffel wind tunnel at LadHyX, see Figure 3, 4 & 5. The square test section is 180 mm wide. The profile is allowed to oscillate in flexural-torsional motions. The airfoil has a chord c=0.12 m and a span width b=0.17 m. The rotation centre O is located at the forward quarter chord and the gravity centre G is at the distance d behind O. The mean angle of attack is set to zero. Sand grains are glued near the leading edge in order to trigger the boundary layer laminar-turbulent transition always at the same place during the experiments. Two end plates are mounted at the extremities in order to further a 2D flow.

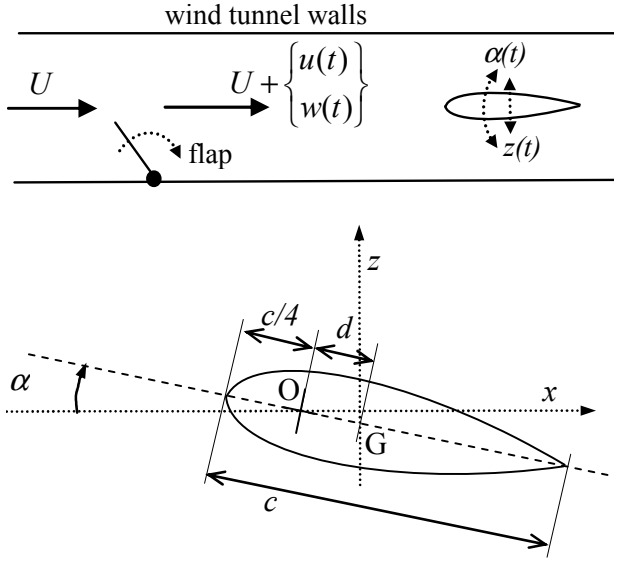

Figure 3: *Principle of the experiments and airfoil geometrical parameters.*

Dynamics of the system is set by means of springs for flexion and torsion, as sketched Figure 4. Special care has been taken to minimize the structural damping of the system: especially no bearings are involved in the design, thus avoiding any friction between moving parts. The non linear feature is provided on the flexion stiffness by two linear contact springs which respond only if the amplitude is larger than a gap value.

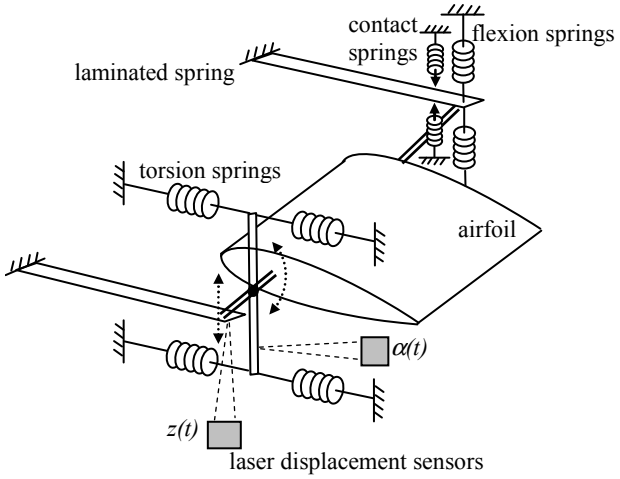

Figure 4: *Kinematics of the flexible airfoil.*

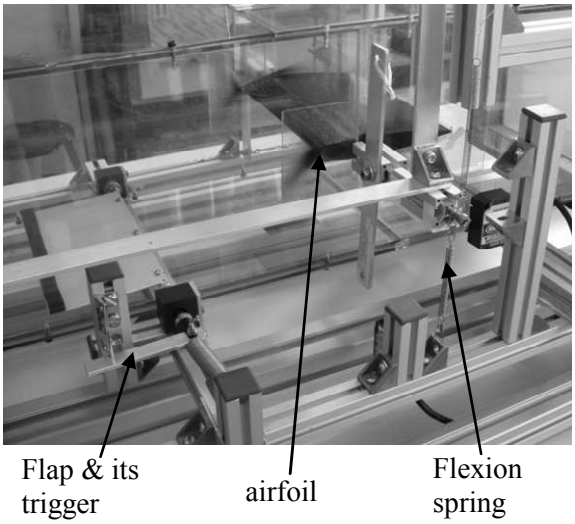

Figure 5: *General view of the system in wind tunnel test section.*

The initial perturbation is provided by a flap mounted on the wind tunnel floor upstream the profile, as presented Figure 3. The length of the flap is 45 mm and 170 mm wide. The rotation axis of the flap is located 160 mm upstream the wing rotation axis. By using a tensioned spring which is suddenly released, the flap generates a short impulse $\{u(t), w(t)\}$ which adds to the upstream wind velocity U. This perturbation has been identified with two components hot wire anemometry for later investigation and comparison

with mechanical modelling.

Typically, the flap generates a transient short impulse on the wind velocity, leading to a unique peak of +20% (referred to U) on longitudinal component u, and simultaneously two peaks on vertical component w of -15% and +30% respectively. Time duration of the perturbation is around 0.05 second, well below the eigenperiod of the two airfoil degrees of freedom.

2.2 Measurement techniques

The reference wind velocity U is measured with a Pitot tube connected to a manometer. A thermocouple measures the ambient temperature for correcting the reference wind velocity. Typical Reynolds number of the experiments, based on the chord, is in the range 80 000 – 120 000.

The two motions are measured with two laser displacement sensors which the output signals are connected to a high speed acquisition and signal processing device. The physical variables z and α versus time are provided by recombination of the measured signals following the system kinematics.

An initial instant reference is deduced by using the signal from an accelerometer mounted on the flap. It is also used to trigger the measurements.

All these signals are connected to an acquisition system PAK provided by Mueller-BBM. It consists mainly of a 24 bits and 8 channels acquisition card and a signal processing software. Typical duration of acquisition is 10 s with a sampling frequency 8192 Hz.

2.3 Identification of parameters

The equations of motion read (Fung, 1993)

$$\begin{aligned} m\,\ddot{z} + 2m\eta_z\,\omega_z\,\dot{z} + k_z\,z + m\,d\,\ddot{\alpha} &= F_z \\ J_O\,\ddot{\alpha} + 2J_O\,\eta_\alpha\,\omega_\alpha\,\dot{\alpha} + k_\alpha\alpha + m\,d\,\ddot{z} &= M_O \end{aligned} \quad . \tag{1}$$

The eigenvalues for the non-coupled case (d=0) are

$$\begin{aligned} \lambda_\alpha &= \omega_\alpha{}^2 = (2\pi f_\alpha)^2 = k_\alpha / J_O \\ \lambda_z &= \omega_z{}^2 = (2\pi f_z)^2 = k_z / m \end{aligned} \tag{2}$$

For the more general coupled case, it can be shown that the distance d between the centre of gravity and the axis of rotation modifies the eigenvalues so that

$$\lambda_1 + \lambda_2 = (\lambda_z + \lambda_\alpha)\frac{1}{1 - md^2/J_O} \tag{3}$$

where the eigenvalues of the coupled system are λ_1 and λ_2.

The structural parameters are determined without wind. First we deal with the two motions separately. We measure the natural frequencies f_α and f_z by spectral analysis and the stiffness k_α and k_z by static calibration. Then we deduce the inertia J_O and m from equations (2).

The frequencies f_1 and f_2 of the coupled system are then measured and the distance d is deduced from equation (3).

The linear aerodynamic loads can be modeled using Scanlan's flutter derivatives (1977)

$$\begin{aligned} F_z &= \frac{1}{2}\rho bcU^2\left(H_1\,\frac{\dot{z}}{U} + H_2\,\frac{\dot{\alpha}c}{U} + H_3\,\alpha + H_4\,\frac{z}{c}\right) \\ M_O &= \frac{1}{2}\rho bc^2U^2\left(A_1\,\frac{\dot{z}}{U} + A_2\,\frac{\dot{\alpha}c}{U} + A_3\,\alpha + A_4\,\frac{z}{c}\right) \end{aligned} \tag{4}$$

where the flutter derivatives, or aeroelastic coefficients, can be expressed with the help of Unsteady Airfoil Theory (UAT), (Fung 1993). Here we calculate the pure aerodynamic damping terms H_1 and A_2, making the quasi-steady assumption (QST) (Hémon 2006), so as

$$H_1 = \frac{-1}{U}C_z{}' ; \qquad A_2 = \frac{-1}{8}\frac{c}{U}C_z{}' \quad . \tag{5}$$

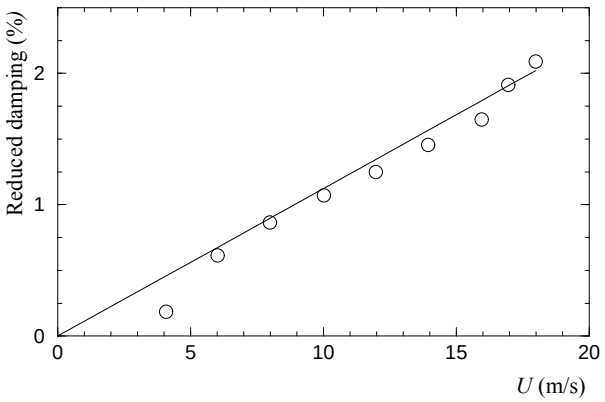

Figure 6: *Aerodynamic damping of flexion versus velocity; (○) experiment; (-) QST.*

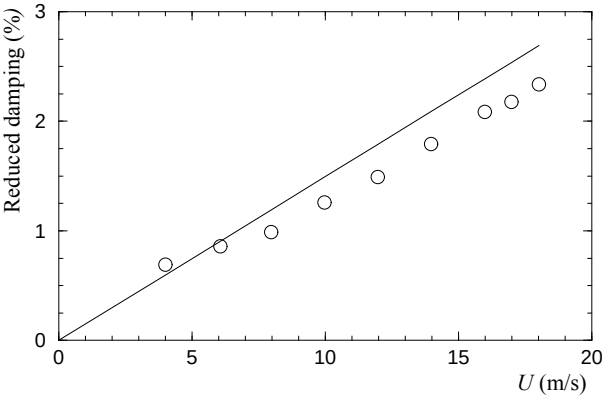

Figure 7: *Aerodynamic damping of torsion versus velocity; (○) experiment; (-) QST.*

Comparison with experimental values, using the

lift derivative $C_z' = 2\pi$, is given in Figure 6 and 7 for flexion and torsion respectively. Good agreement is obtained which validates the experimental setup and the structural parameters identification procedure.

The total energy is the sum of kinetic and potential energy which reads:

$$E(t) = \frac{1}{2} m\, \dot{z}^2(t) + \frac{1}{2} J_O\, \dot{\alpha}^2(t) + m\, d\, \dot{\alpha}(t)\, \dot{z}(t) + \frac{1}{2} k_z\, z^2(t) + \frac{1}{2} k_\alpha\, \alpha^2(t) \quad (6)$$

This quantity will be used to quantify transient growth. It will be nondimensionlized by the initial energy E_0 determined from the initial conditions. The maximum value of *E(t)*, as observed from the time series, will be denoted E_{max}.

All the measured parameters of the flexible system are given in Table 1 of section 4.

2.4 Identification of non linear parameters

The non linearity is located on the stiffness of the flexion due to the contact springs. Two parameters are needed, the gap z_{nl} between the position zero and the contact, and the resulting stiffness $k_{nl} = k_z + \delta k_{nl}$ above this gap.

The calibration is performed statically. This leads to a value z_{nl} = 0.655 mm and a stiffness $\delta k_{nl} = 0.14\, k_z$. The non linear feature of the flexural stiffness leads to an additional term on the energy that reads:

$$E_{nl}(t) = \frac{\delta k_z}{4} \left(\begin{array}{c} \left(|z - z_{nl}| + (z - z_{nl})\right)^2 + \\ \left(|z + z_{nl}| - (z + z_{nl})\right)^2 \end{array} \right) \quad (7)$$

This quantity is added to the linear energy (6) when measurements are performed with the non linear system.

3. RESULTS

The experiments are mainly performed by comparison between linear and non linear behaviour. The first measurements are the frequencies of the system, and their evolution versus the wind velocity, which is presented in figure 8.

The non dimensional velocity parameter $1 - U/U_c$ is introduced as in (Schmid & de Langre 2004) where the linear critical velocity U_c is previously estimated by experiments.

Linearly at the onset of flutter, the two initial frequencies coalesce in one. In non linear case, the coalescence of the two frequencies occurs at a velocity U_{cnl} which is lower than in linear case. Then for a velocity just above U_{cnl} and below U_c the conditions for a by-pass transition to flutter are present.

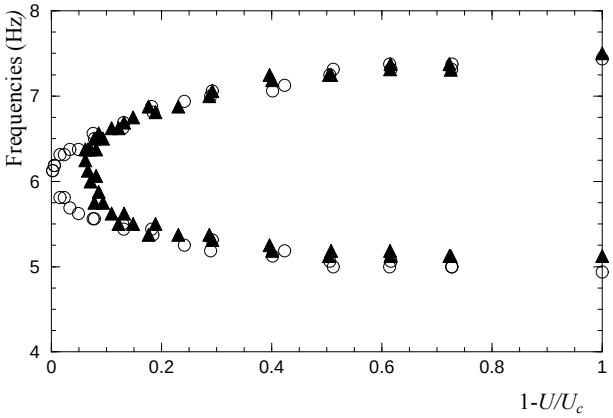

Figure 8: *Frequencies of the 2 modes versus velocity parameter; (○) linear; (▲) non-linear.*

Now the transient growth of energy is measured. The test procedure is as follow:

- The flap is prepared in position with its torsion spring,
- The wind tunnel velocity is adjusted to the desired value,
- The flap is released manually and the accelerometer, which is mounted on it, triggers automatically the measurements,
- After recording, the time history of total energy of the system is computed and plotted,
- The initial value E_0 and the maximum E_{max} are read.

All these data are collected and finally presented in figure 9, for linear and non linear cases. The amplification reaches a level 9 times the value of initial energy for linear system just before critical velocity.

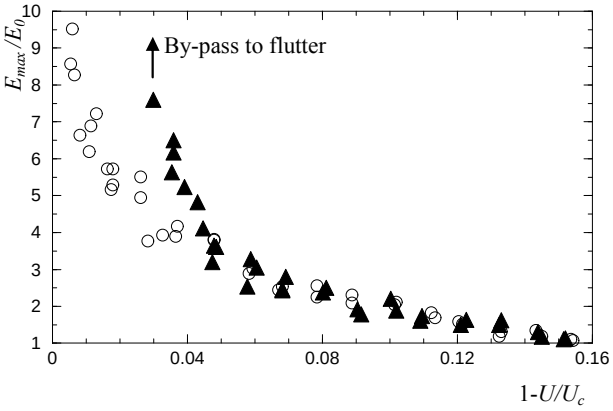

Figure 9: *Amplification rate of energy versus velocity parameter; (○) linear; (▲) non-linear.*

With the non linear system, the behaviour follows the evolution of the linear system for low velocity. Then, approaching the value U_{cnl}, the energy growth rate increases more rapidly than in linear case, and finally transition to flutter occurs, after an amplification larger than 7.

The comparison between linear and non linear behaviour is essential for the confirmation of the by-pass transition due to transient growth, because this is not a simple by-pass transition by initial amplitude effect. We must show indeed that the initial perturbation produced by the flap generates an energy which remains under the level of the energy for which the non linear behaviour occurs, i.e. that the coordinate z remains under z_{nl} at the initial instant.

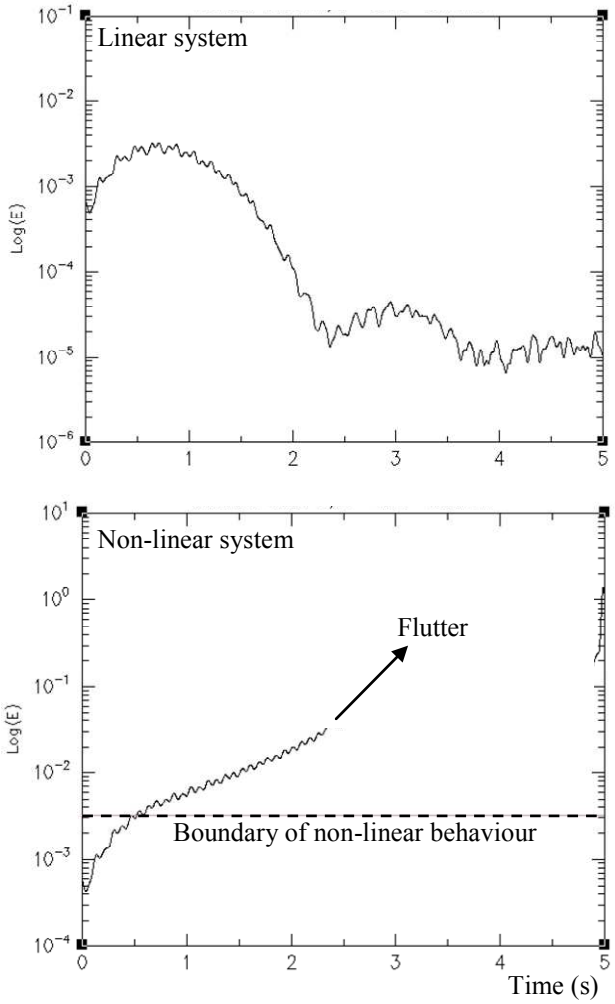

Figure 10: *Energy time histories in linear and non-linear cases at U/U_c=0.99.*

This is shown in figure 10 where we present time histories of the total energy in linear and non linear cases. Wind velocity is just below the linear critical velocity: the system is stable for the linear case, and by-pass transition to flutter occurs for the non linear case. For the latter, the boundary of the non linear behaviour is determined statically. This energy level corresponds to the potential energy when the system reaches the coordinate z_{nl} upper which the non linear springs are involved.

This figure shows that the initial energy generated by the flap is well below the non linear boundary, and that the transient growth is responsible for transition to flutter indeed.

Further investigations are currently performed in order to simulate numerically the mechanism, taken into account the upstream wind velocity perturbation generated by the flap.

4. NOMENCLATURE

F_z	lift force (N)
M_O	Aerodynamic momentum about O (N.m)
b, c	span and chord of the profile (m)
d	distance between gravity centre and O (m)
$E(t)$	total mechanical energy (J)
E_0	initial mechanical energy (J)
E_{max}	maximum of the mechanical energy (J)
f_α f_z	frequencies of pure motions (Hz)
f_1 f_2	frequencies of the coupled motion (Hz)
J_O	inertia about O (kg.m^2)
k_α k_z	stiffness (N.m/rad) and (N/m)
m	mass involved in the vertical motion (kg)
U	wind velocity (m/s)
U_r	reduced velocity ($U_r = U/c\,f_z$)
z	vertical displacement (m)
z_{nl}	gap for non linear case (m)
α	torsion angle about O (rad)
δk_{nl}	nonlinear torsion stiffness (N.m/rad)
η_α η_z	reduced structural damping (%)
λ_α λ_z	eigenvalues of pure motions (rad.s^{-2})
λ_1 λ_2	eigenvalues of the coupled motions (rad.s^{-2})

m	0.951	
J_0	8.736E-04	
k_α , k_z	1.6599	880.7
z_{nl}	0.000655	
δk_{nl}	120	
b, c	0.12	0.17
f_α , f_z	6.9375	4.9375
f_1 , f_2	4.9375	7.4375
d	0.0093	
η_α , η_z	0.2	0.15

Table 1: Values of system parameters.

5. REFERENCES

Fung, Y.C., 1993, An introduction to the theory of aeroelasticity. Dover, New York.

Hémon, P., de Langre, E. & Schmid, P., 2006, Experimental evidence of transient growth of energy before airfoil flutter. *Journal of Fluids and Structures*, **22**: 391-400.

Hémon, P., 2006, Vibrations des structures couplées avec le vent. Editions de l'Ecole Polytechnique.

Lee, Y.S. et al., 2005, Triggering mechanisms of limit cycle oscillations due to aeroelastic instability. *Journal of Fluids and Structures*, **21**: 485-529.

Marsden, C.C., Price, S.J., 2005, The aeroelastic response of a wing section with a structural freeplay nonlinearity: An experimental investigation. *Journal of Fluids and Structures*, **21**: 257-276.

Scanlan, R. H., Tomko, J. J., 1977, Airfoil and bridge deck flutter derivatives. *ASCE Journal of the Engineering Mechanics Division*, December, 1717-1737.

Schmid, P. & de Langre E., 2003, Transient growth before coupled-mode flutter. *ASME Journal of Applied Mechanics*, **70**: 894-901.

Schmid, P. & Henningson D.S., 2001, Stability and transition in shear flows. Springer, New York.

Acknowledgements

This research work is supported by AIRBUS France under the program Wing Flutter (WINFLU).